Test Tools for Transarterial Chemoembolization Simulation

RYAN CARROLL, BENJAMIN ENGEL, ERIC PRINTZ, JUSTIN SCHMIDT

Biomedical Engineering Department, University of Wisconsin - Madison

Abstract—Liver cancer in various forms is a major cause of mortality worldwide and current treatment methods are highly ineffective. Transarterial chemoembolization (TACE) is a chemotherapy delivery technique which improves the localization of treatment. Currently, TACE is guided through X-ray imaging but would benefit from the use of real-time 3D MRI guidance. The purpose of this project was to create a set of test tools to allow for the development and testing of MRI guided transarterial chemoembolization. In phase I a liver phantom was created which allows physicians to practice liver catheterization under MRI guidance. Phase II requires similar testing using porcine test subjects. In phase II of this project a test subject transport device was created which allows the animal test subject to be transported from the MRI scanner to an X-Ray machine for catheter placement verification. The phantom successfully achieved flow in all vessels and was imaged using VIPR (vastly under-sampled isotropic projection reconstruction) and fast gradient echo pulse imaging sequences. The transport device was successfully tested to verify that catheter movement was under the specified 0.5 inch tolerance. The device was also tested under loads to verify that it is capable of supporting 2.91 times the weight of the maximum animal test subject with less than 0.25 inches of deflection.

Keywords—Transarterial Chemoembolization (TACE), MRI guided catheterization, X-ray digital subtraction angiography (DSA), Couinaud segment

INTRODUCTION

Primary liver cancer and hepatic metastases of the liver represent a significant medical problem throughout the world. The liver is the most common site of metastatic tumor deposits in the body and hepatic metastases represent a major cause of mortality in patients with other malignant tumors.[1] Hepatic metastases are common in the case of both colorectal and breast cancer. In 20-30% of colorectal cancer cases, the liver is the only site of metastases. Hepatic involvement in almost all forms of cancer is often indicative of a life threatening illness.[2] Depending on the primary site of cancer, 30-70% of patients who die from cancer have liver metastases present in their autopsies.[3] In addition to metastases, primary liver tumors in the form of hepatocellular carcinoma continue to be a major cause of death, especially in Asia.[4] For this reason, effective identification and treatment methods are necessary to improve a patient's chance of survival when diagnosed with either primary liver cancer or hepatic metastases.

Current Treatment

Current treatment methods for liver cancer in its various forms are highly ineffective. The most promising hope for a cure is surgical resection. Five years after surgical resection of colorectal metastases, 40% of patients are alive, and 30% are disease free. However, in the case of colorectal liver metastases only 20% of all lesions are surgically operable leaving an enormous portion of patients to rely on systemic chemotherapy and radiation treatments.[5] While breakthroughs have been made in the localization of these treatments, systemic treatments continue to be ineffective. The response rate to the most commonly used chemotherapy agent (5-fluorouracil) in the treatment of hepatic metastases worldwide is only 20%. Survival rates for patients with unresected cancer vary based on the origin of the study; however, the following figures give a good indication of the ineffectiveness of systemic treatment: "1-year survival for solitary or limited liver metastases varies from 38 to 83%, whereas 3-year survival for solitary or limited metastases extends from 0 to 33%, and the figures for multiple and diffuse metastases fall between 0 and 4%."[5] In the case of localized liver cancer treatment, transarterial chemoembolization has proven to be more effective than systemic approaches.

Transarterial Chemoembolization (TACE)

Transarterial chemoembolization is a localized administration of both chemotherapeutic drugs and embolizing agents. Cytotoxic drugs kill cells in the area of the cancerous tumor while embolizing agents cause peripheral arterial occlusion restraining the drug to the affected area. Restraining the drug in the location of the tumor effectively increases contact time, prior to the drug's removal by the liver.[6] TACE has been shown to effectively reduce the size of unresectable metastases in 50% of cases.[2] Transarterial chemoembolization is especially effective in highly vascularized regions where tumors promote angiogenesis.[7] The dual blood supply of the liver increases the effectiveness of this procedure. Blood is supplied to the liver via two major sources, the portal vein (25%) and the hepatic artery (75%). Because the peripheral arterial occlusion only decreases at most 25% of the blood flow to the liver, healthy tissue is able to survive on a constant supply of venous blood. Within the liver, the hepatic artery branches into eight separate Couinaud segments, and therefore catheterization procedures can effectively target individual segments.[8] Current administration of chemotherapy and embolizing agent is carried out through a catheterization of the femoral artery to the location of the target area under X-ray guidance.

X-ray DSA/MRI Techniques

Through the use of X-ray digital subtraction angiography (DSA), real time high resolution imaging is possible. This technique, however, falls short of magnetic resonance imaging. In X-ray, the localization of tumors relies entirely

Address correspondence to Benjamin Engel, University of Wisconsin – Madison, Biomedical Engineering Department. M1076 Engineering Centers Building, 1550 Engineering Drive, Madison, WI, 53726. Electronic mail: bengel@wisc.edu

on the uptake of contrast agent to highly vascularized regions, thus tumors are often not visible.[5] Using simple 2D MRI scans, it was determined that the placement of catheters near their target tumors was incorrect in 40% of X-ray guided cases.[9] For this reason, current TACE procedures require a pre-operative CT or MRI scan prior to catheter placement under X-ray guidance. Interventionalists would benefit greatly from three-dimensional MRI images. Magnetic resonance imaging benefits from a very high degree of soft tissue contrast, thus tumors are much more easily visualized in MRI studies. Recent advances in MRI allow three-dimensional imaging to be done in real time. Through the use 3D real-time MRI, interventionalists have the ability to actively guide catheters while visualizing tumor location. A multitude of undersampling techniques make real-time imaging both spatially accurate and temporally feasible.[5] This eliminates the need for a pre-operative CT or MRI scan for tumor localization. Despite the advantages of MRI, most interventionalists are accustomed to using X-ray as a catheter guiding tool and do not utilize MRI for this application. Therefore, significant training is necessary before these interventionalists become comfortable using MRI as a catheter guiding technique.

TACE Test Tools

Two separate test tools are needed to conduct adequate physician training on MRI guided catheterizations. First, an MRI compatible phantom of the arterial liver vasculature will allow catheterization procedures to be practiced on a non living subject. Physicians will guide a catheter to a specific segment of the phantom liver under MRI guidance and verify its position through the use of X-ray DSA. Phase two of this training requires the same procedure to be performed on a porcine subject. Due to the weight of these subjects and the circular shape of the MRI coil in which the subject is imaged, an animal subject transport table is required to perform the physical transition from MRI to X-ray.

METHODS

Liver Phantom

All eight Couinaud segments of the arterial liver vasculature as well as the primary key abdominal arteries were created using Tygon® tubing. Key abdominal arteries included the aorta, femoral arteries, renal arteries, superior mesenteric artery, and the entire celiac trunk. Complex vascular junctions were created by making small holes in the larger of the two vessels and tacking the smaller vessel to that hole at the desired angle. These junctions were secured in place with a hot plastic melt then layered in silicone caulk to ensure a water tight seal. Simple junctions were created using barbed wye connectors. The tubing used for the vessels ranged from an inner diameter of 1/8 in. to 5/8 in. depending on the vessel size.

The created vasculature was suspended within an acrylic enclosure (Figure 1) which serves the purpose to both maintain the vasculature orientation and also to hold a gel material that will be used to mimic the MRI imaging characteristics of the surrounding abdominal tissue. The enclosure was made from 3/8 in. thick acrylic sheeting and measures 14.75 in. by 14.75 in. by 8.75 in. creating the correct inside dimensions. The five sides of the enclosure (excluding the top) were adhered together using acrylic cement. Silicone caulk was used to line the inside of all edges ensuring a tight seal. A removable cover was made from 3/8 in. acrylic and measured 14.75 in. by 14.75 in. to fit exactly over the top of the enclosure. The top sides of the enclosure were lined with a waterproof seal. Four MRI compatible latches were used to firmly hold the cover down against the seal.

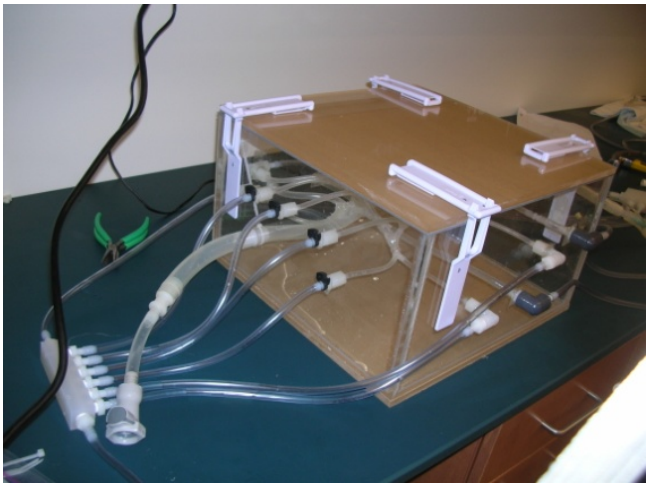

FIGURE 1. Photo of liver phantom highlights multiple design features including acrylic phantom enclosure, removable acrylic top, Tygon® liver and abdominal vascular network, vinyl fluid return lines, and polyethylene fluid manifolds.

Holes were drilled in the side of the acrylic enclosure to accompany barbed elbow connectors which connected the vasculature to vinyl fluid return lines. These connectors were appropriately glued into the pre-drilled holes using a quick setting epoxy. The fluid return lines connected the vasculature to two separate polyethylene fluid manifolds and eventually the fluid reservoir housed in the MRI control room. These manifolds served to reduce the number of tubes required to return fluid to the reservoir. Half of the vessels were connected to each of the manifolds. Each manifold consisted of seven inflows and one outflow that returns fluid back to reservoir mentioned above. The singular outflows from each manifold were fitted with quick disconnect couplings with shut off capabilities for interfacing with the current fluid pump setup.

Flow is provided to this network by a peristaltic Masterflex® pump (model number: HV-77521-40) equipped with a Masterflex® pump head (model number: HV-77250-62). The pump is fitted with a serial interface that allows programmable flow control to be implemented later in the project. The pump currently provides constant flow through the system at variable flow rates with a maximum achievable flow of 3 L/min. This constant flow can be adjusted via a knob on the front of the pump.

A catheter insertion point was incorporated into the external tubing system to allow physicians and other

researchers to insert a catheter and guide-wire into the vasculature via the right femoral artery. The femoral artery is where the majority of TACE procedures are initiated and provides a realistic situation for those using the phantom. Catheters are used in TACE procedures, but can also be used by researchers to inject contrast agent and saline into the phantom for imaging purposes. The junction between the catheter port and the tubing was made air-tight so that outside air was not introduced to the system causing image artifact during the scans.

Animal Subject Transport Table

The subject transport table is used to aid in the transport of porcine subjects within the MRI coil from the MRI to the X-ray machine to verify catheter placement in the liver. The table must be designed to match the curvature of the MRI couch and the flat X-ray table. The table was created from high density polyethylene (HDPE) because its attenuation property is less than that of the PVC coil. This ensures that the transport table does not restrict the imaging capabilities of the X-ray DSA unit. The base of the table was made out of 0.5 in. HDPE and cut to the dimensions 48 in. by 15.5 in, allowing it to fit to the width of the MRI couch as well as support the entire length of the porcine subject. Handles were included in the design of the table to aid in the maneuverability during transport. The handles are centered in the middle of the table at a distance of 26 in. from each other and 1.5 in. from the sides of the table. To make sure all hand sizes are able to fit inside of the handle, the width of the handles were cut to 5 in. wide.

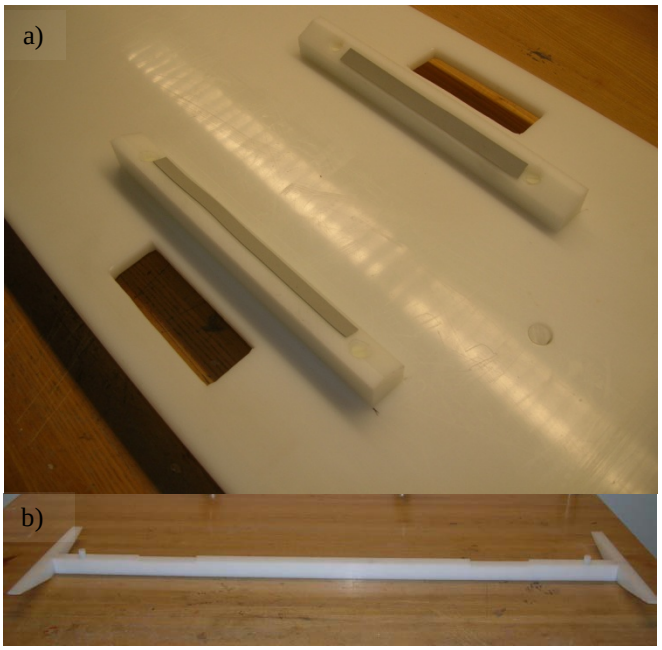

FIGURE 2. Series of photos illustrates features of animal subject transport table. a) Photo highlights coil support rails with silicone rubber backing, handles for ease of transport, and holes for interface with MRI couch adapter. b) Photo shows MRI couch adapter used to adapt animal subject transport table to curvature of the MRI couch.

Four rails were fastened to the base of the table to prevent any movement of the coil during transport. These rails measured 1 in. by 1 in. by 10 in. and one corner was cut to a 28 degree angle to fit to the curvature of the coil. The rails were fastened to the table using nylon bolts that were drilled through the table. On the bottom of the table the nuts were recessed into the table so that they did not protrude. This allowed the table to sit evenly on the flat surface of the X-ray table. Rubber stripping was applied to the surface of the rails to further create friction between the coil and the rail and to prevent any rolling or sliding of the coil during transport. Nylon straps were used to fasten the coil to the table during transport. Plastic latches were used to secure the straps. These straps wrapped through the handles, under the table and around the top of the coil.

Due to the curvature of the MRI couch, an adapter was used to fit the table to this curvature. Two pieces which matched this curvature were cut out using a template. A long support member with a length of 40 in. was placed between these pieces they were fastened to the support member with brass screws. The height of the support member and curvature pieces is 0.6 in. which is the distance from the bottom of the table to the base of the MRI couch. The adapter was fitted with two 0.5 in. diameter rods on its top surface which fit directly into holes drilled out of the bottom of the table allowing the adapter to be securely attached to the table. This prevents movement of the table while the MRI couch enters and exits the MRI bore.

Testing

Prior to imaging with the liver phantom, the phantom was tested for potential leaks and sufficient flow in each vessel. These tests were performed by filling the phantom enclosure with water and pumping fluid through the vascular network at a rate of 3 L/min. A video was taken to assess the flow in each vessel. Vessel leakage was assessed by observing whether or not red dye passed from the vasculature into the surrounding water within the enclosure.

The phantom was then imaged using MRI to assess the phantom's imaging capabilities. The phantom was imaged using two different MRI pulse sequences. The first pulse sequence was a fast gradient echo pulse sequence. The sequence parameters were TE = 2ms, TR = 20ms, NEX = 2, 128 x 128 resolution. The scan was performed on a GE Healthcare 1.5T MRI scanner. The sequence produced a 3D image of the phantom which was used to verify that sufficient signal was received from each vessel. Verification was done by inspecting the resulting 3D image for signal voids due to material artifacts or air-water interface artifacts.

The second MRI image was acquired using the vastly under-sampled isotropic projection reconstruction (VIPR) pulse sequence. Similar to the fast gradient echo pulse sequence, this sequence also resulted in a 3D image of the phantom. However, this sequence is flow sensitive and was used to determine if flow was achieved in each vessel. Contrast was injected into the vasculature to improve contrast and flow was provided at a rate of 3 L/min during the scan.

The transport table was tested for changes in catheter position during transport as well as for its weight capacity. Weight capacity was tested in two manners. The first test was performed to verify that table was able to hold at least the weight of the largest porcine test subject (132 lbs.) under proper use. To perform this test, the transport table was supported under each of the four handles. A string was placed across the top of the table which was indicative of the table under zero deformation. Weights were placed on the table in increments of 50 lbs. and vertical deflection was measured as the difference in position between the top of the table and the string. The predetermined vertical deflection tolerance was 0.25 inches. A similar procedure was performed to simulate misuse of the table. In this test the table was supported at its ends mimicking the act of picking up the table without use of its handles. The same vertical deflection tolerance was used and weights were added in increments of 10 lbs. The same measurement was made.

The second test for the transport table was performed to determine the amount of linear catheter movement which occurs during transition from the MRI unit to the X-ray DSA unit. The tolerance for catheter movement during this test was determined to be 0.5 in. Because a porcine test subject was not available, these tests were performed using the liver phantom as the test subject filled with 50 lbs. of water or approximately 6.2 gallons. The first series of transports were performed on the phantom without the use of the transport table. This was the experiment control. The catheter was placed within the phantom and the unit was transferred from the MRI to the X-ray machine. The second series of transfers involved the same procedure with the phantom secured to the subject transport table. Finally the third series of transfers was performed with the phantom secured to the subject transfer table with the catheter immobilized and taped to the table. Each series included 10 trials. Linear catheter movement was measured at the catheter insertion point on the phantom after each transport was performed.

RESULTS

Careful analysis of video footage from the red dye procedure indicated that dye was not able to pass through the vascular junctions and into the surrounding fluid. This indicated that the vasculature was watertight and allowed no leakage when flow was administered at its maximum rate. Red dye adequately diffused through all the regions of the vasculature within 3 seconds indicating that all of the vessels achieved required flow. This test demonstrated that it was safe for the device to be imaged.

The MRI scans using the fast gradient echo pulse sequence showed that sufficient signal was received from all parts of the vasculature. This result was found by comparing the scan images with still images of the vasculature. Each branch of the vasculature was labeled in the scan image to aid the comparison. All branches were present in the MRI image indicating that no sector of the phantom suffered from material or air-water interface artifacts.

Scans performed using the VIPR pulse sequence further indicated that adequate flow was achieved in all eight Couinaud segments as well as the key abdominal arteries. This was evident as all vessels appeared in the VIPR image with smaller vessels appropriately appearing less prominently due to decreased flow based on vessel size.

The results of the deflection tests performed on the subject transport table were plotted as distance displaced versus weight applied, which yielded the graphs seen below. Physically, only 250 pounds could be placed on the device given its size. Additional points past this threshold were extrapolated using a regression to reach the deflection threshold of 0.25 in. Linear, order two polynomial, and exponential regressions were formulated on the current points using Microsoft Excel. Then each regression equation was used to plot the theoretical points used to estimate further deflection. These points were visually inspected to assess their fit with the experimental data. This evaluation was employed to reduce the chance of over fitting the experimental data. After performing the evaluation it was clear that the data exhibited a linear trend in the case of the normal use and a polynomial trend in the case of misuse. From this our safety factors could be calculated as follows:

$$Safety\ Factor = \frac{W_{Threshold}}{W_{MaxPig}}$$

$W_{Threshold}$ is the weight the table was capable of supporting at the threshold value of deflection. W_{MaxPig} is the maximum weight of the pig (132 lbs). The safety factors were then found to be 2.91 during proper use and 0.05 during misuse.

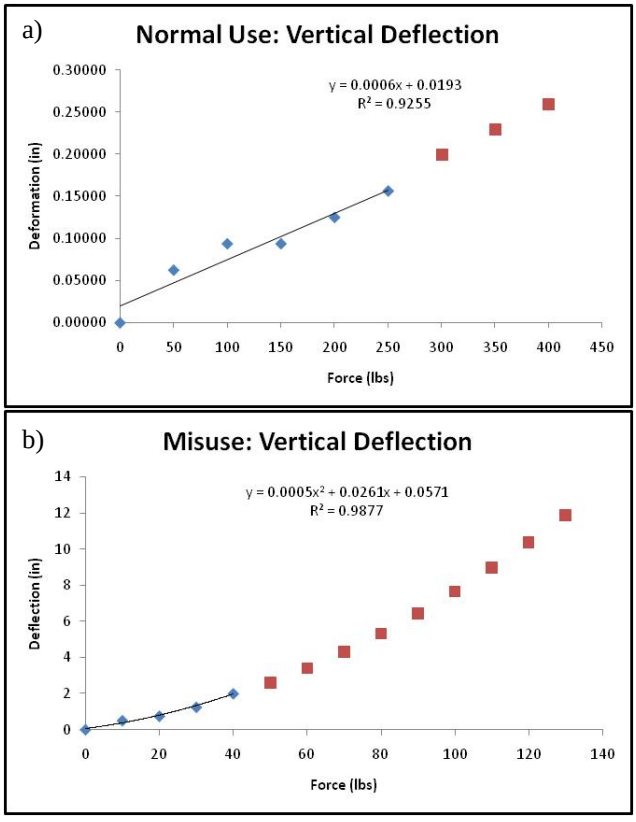

FIGURE 3. a) Graph shows deflection (in.) plotted against applied force (lbs.) for proper use of the device. Measured points can be seen in blue and extrapolated points can be seen in red based on the equation shown. b) Graph shows similar chart indicating deflection under misuse.

The ability of the transport table to support 2.91 times the weight of the maximum test subject during proper use and only 0.05 times the weight of the maximum test subject during misuse illustrates the importance of proper use.

The results of the subject transport tests indicated that catheter movement was not problematic in the case of subject transport from the MRI unit to the X-ray DSA unit. In all 10 trials performed in all three different situations, zero linear catheter movement was recorded. Although this result could be indicative that the catheter will never move during a transfer, additional factors should be considered when moving a biological subject instead of a phantom. The biological subject could have different internal characteristics that result in the catheter being more subject to movement. This should be considered when performing additional tests in the future.

CONCLUSION

Testing indicated that the developed TACE simulation test tools meet specifications and will prove effective in the advancement of MRI guided TACE procedures. The phantom demonstrated strong imaging characteristics. This will allow for physicians to immediately begin training on MRI guided catheterization procedures using this device; the first step in the advancement of the procedure. Testing also indicated the efficacy and safety of the animal subject transport device. This device is crucial in the second phase of the study which aims to prove the efficacy of MRI guided TACE procedures by physicians using living test subjects.

The ultimate goal of the MRI guided TACE research and physician training using these tools is to prove the effectiveness of MRI guided catheterization procedures in general. The TACE procedure has been studied extensively and is very common in treating liver metastases. TACE will be used in conjunction with the test tools developed to introduce and train physicians on MRI guided catheterizations. With the success of TACE under MRI guidance, additional procedures will begin to take advantage of the superior catheter guidance offered by MRI.

ACKNOWLEDGEMENTS

We would like to thank Wally Block, PhD and Ethan Brodsky, PhD for their guidance throughout the entirety of this project. We would also like to thank William Murphy, PhD for advising and overseeing the completion of this project. Finally, we would like to thank the National Cancer Institute for funding this work through our client Wally Block PhD (Grant NCI1 RO1-CA116380)

REFERENCES

[1] Vogl T, Muller, P, Mack, M, Straub, R, Engleman K, and Neuhaus P. Liver metastases: Interventional therapeutic techniques and results, state of the art. *Eur Radiol* 1999; 9: 675-684.

[2] Vogl T, Mack M, Balzer J, Engelman K, Straub R, Eichler K, Woitaschek D, and Zangos S. Liver Metastases: Neoadjuvant Downsizing with Transarterial Chemoembolizationbefore Laser Induced Thermotherapy. *Radiology* 2003; 229: 457-464.

[3] Nawaz, A, Macdonald S, Tam, E, Sherlock, D, Sheen A, and Punter, M. Hepatic chemoembolization. http://www.emedicine.com

[4] Block, WF. 3D Real-Time MRI Imaging Grant. PHS 398/2590.

[5] Stangl R, Altendorf Hofman A, Charnley RM, and Schede J. Factors influencing the natural history of colorectal liver metastastes. *Lancet* 1994, 343:1405-1410.

[6] Vogl, T, Naguib, N, Nour-Eldin, A, Rao, P, Emami, A, Zangos, S, Nabil, M, and Abdelkader, A. Review on transarterial chemoembolization in hepatocellular carcinoma: Palliative, combined, neoadjuvant, bridging, and symptomatic indications. *Eur. Radiol.* 2008; Oct 1, Pre print

[7] Lopez RL, Pan S, Lois J, McMonigle M, Hoffman A, Sher L, Lugo D, and Makowka L. Transarterial chemoembolization is a safe treatment for unresectable hepatic malignancey. *Am Surg* 1997, 63:923-926.

[8] Chiandussi L, Greco F, Sardi G, Vaccarino A, Ferraris CM, Curti B. Estimation of hepatic arterial and portal venous blood flow by direct catheterization of the vena porta through the umbilical cord in man: preliminary results. Acta Hepatosplenol 1968; 15:166-171.

[9] Vogl TJ, Balzer JO, Mack MG, Bett G, Oppelt A. Hybrid MR interventional imaging system: combined MR and angiography suites with single interactive table. Feasibility study in vascular liver tumor procedures. Eur Radiol 2002; 12: 1394-1400.